IFT-UAM/CSIC-10-18
EURONU-WP6-10-16

A minimal Beta Beam with high-Q ions to address CP violation in the leptonic sector

P. Coloma[a,b], A. Donini[b,c], P. Migliozzi[d], L. Scotto Lavina[e], F. Terranova[f]

[a] Dep. Física Teórica, Universidad Autónoma de Madrid, 28049 Madrid, Spain
[b] I.F.T., Universidad Autónoma de Madrid/CSIC, 28049 Madrid, Spain
[c] I.F.I.C., Universitat de Valencia/CSIC, 46071 Valencia, Spain
[d] I.N.F.N., Sez. di Napoli, Napoli, Italy
[e] University of Zurich, Physik-Institut, CH-8057 Zurich, Switzerland
[f] I.N.F.N., Laboratori Nazionali di Frascati, Frascati (Rome), Italy

Abstract

In this paper we consider a Beta Beam setup that tries to leverage at most existing European facilities: i.e. a setup that takes advantage of facilities at CERN to boost high-Q ions (^{8}Li and ^{8}B) aiming at a far detector located at $L = 732$ Km in the Gran Sasso Underground Laboratory. The average neutrino energy for ^{8}Li and ^{8}B ions boosted at $\gamma \sim 100$ is in the range $E_\nu \in [1, 2]$ GeV, high enough to use a large iron detector of the MINOS type at the far site. We perform, then, a study of the neutrino and antineutrino fluxes needed to measure a CP-violating phase δ in a significant part of the parameter space. In particular, for $\theta_{13} \geq 3^\circ$, if an antineutrino flux of 3×10^{19} useful ^{8}Li decays per year is achievable, we find that δ can be measured in 60% of the parameter space with 6×10^{18} useful ^{8}B decays per year.

PACS: 14.60.Pq, 14.60.Lm

1 Introduction

After several years of design and construction, a new generation of experiments at accelerators (T2K [1], NOVA [2]) and reactors (Double-Chooz [3], Daya-Bay [4], RENO [5]) is about to explore *subdominant* leptonic mixing at the atmospheric scale, i.e. oscillations beyond leading $\nu_\mu \to \nu_\tau$ transitions at energies and baselines where the oscillation frequency mainly depends on the mass-squared difference $|\Delta m^2_{13}| \simeq |\Delta m^2_{23}|$. At this scale, $\nu_\mu \to \nu_\tau$ transitions are driven by the large θ_{23} angle ($\theta_{23} \simeq 45^\circ$ [6]) while subdominant $\nu_\mu \to \nu_e$ transitions are suppressed by the smallness of the θ_{13} mixing angle between the first and third family. The actual size of θ_{13} is currently unknown and the angle is bounded from above ($\theta_{13} < 11.5^\circ$), especially by former reactor data [7, 8] (see, however, Ref. [9] to see some dependence of the upper bound on θ_{13} due to the CP-violating phase δ from atmospheric data). Three family fits [10] and, particularly, a slight tension between the SNO and Kamland data [11] suggest, however, that θ_{13} might be close to current limits. The above-mentioned experiments will be able to probe values of θ_{13} down to about 3° [12] in 3-5 years from now, and so confirm or disprove this hint for a non-vanishing θ_{13}.

Evidence for $\nu_\mu \to \nu_e$ transitions at the atmospheric scale would be a major breakthrough in neutrino physics: since the ratio $\Delta m^2_{12}/|\Delta m^2_{23}|$ is not exceedingly small ($\simeq 1/30$), a sizable θ_{13} implies that $\nu_\mu \to \nu_e$ oscillations at the atmospheric scale are heavily perturbed by three family interference effects. As a consequence, precision measurements of $\nu_\mu \to \nu_e$ oscillation and its CP-conjugate $\overline{\nu}_\mu \to \overline{\nu}_e$ using artificial sources at long baselines become an ideal tool to address CP violation in the leptonic sector [13].

Distilling CP-violating effects from the rate of appearance of ν_e and $\overline{\nu}_e$ is a tremendous challenge, clearly out of reach for the next round of experiments [14]. The design of a further generation of facilities specifically aimed to probe CP violation in the leptonic sector, to perform precision measurement of the θ_{13} angle and, possibly, to establish the sign of Δm^2_{23} through the exploitation of matter effects has been at the focus of a decade-long study, which was recently summarized in the "International Scoping Study of a Future Neutrino Factory and Superbeam facility" Report [15, 16, 17]. Generally speaking, these facilities require either the construction of underground laboratories of unprecedented size to host massive low-density detectors - as for the options based on "Superbeams" [16] - or of a new major acceleration complex - as for the case of the "Neutrino Factories" [17]. The only notably exception to this scheme pertains to a sub-class of options based on the Beta Beam concept [18], sometimes called "high-energy Beta Beams". Since its inception [19], Beta Beams have been designed with the aim of leveraging at most existing facilities and, in particular, the CERN acceleration complex. As explained in Sec. 2 and 3, Beta Beams that are able to accelerate radioactive ions to high energies and produce multi-GeV ν_e and $\overline{\nu}_e$ allow for the use of high-density detectors, which, in turn, might be hosted in moderate-size underground laboratories. For a CERN-based Beta Beam, the natural option to host the far detector is a laboratory located at a distance $O(600 - 700)$ Km from the neutrino source. The facility that *exploits at most existing European infrastructures*, as discussed in Sec. 3, is a multi-GeV Beta Beam based on the CERN-SPS accelerator pointing to a massive, high-density detector located in one of the experimental halls of the Gran Sasso laboratories. The next cheapest alternative could be represented by the Canfranc Underground Laboratories in Spain, where some engineering would be however needed (albeit not so impressive as for a Mton class Water Čerenkov detector).

The physics performance of this facility and the minimum requests to the accelerator complex to establish CP violation in the leptonic sector in case of positive result from T2K, NOVA or the reactor experiments is at the focus of the present paper (Sec. 4 and 5). Beside the huge practical interest of exploiting in an optimal manner all European facilities without additional infrastructure investment [20], this detailed assessment is particularly relevant at present times: since 2009, machine studies for the Beta Beam are concentrated on facilities that accelerate ions with Q-values larger than originally envisioned ($Q \sim 13$ MeV for ^{8}Li and ^{8}B, to be compared with $Q \sim 3$ MeV for

the ions considered in the original design, ^{6}He and ^{18}Ne) using the existing SPS machine [21, 22]. This option ideally fits the "minimal" scheme mentioned above provided that neutrinos are pointed toward the underground halls of LNGS. Other options either based on low density detectors and/or on new terminal boosters at larger energies than the CERN-SPS have also been studied in literature: for details, we refer the reader to Ref. [18] and, in particular, to Refs. [23, 24, 25] for low-Q ions accelerated by the SPS, Refs. [26, 27, 28, 29, 30, 31] for high-γ Beta Beams (using facilities different from the SPS to accelerate ions) and Refs. [32, 33, 34, 35, 36, 37, 38, 39, 40, 41, 42, 43, 44] for high-Q Beta Beams (either at low-γ and high-γ).

2 Beta Beams with high-Q ions

In order to overtake the intrinsic limitation of ν_μ beams originating from the decay-in-flight of pions, novel sources based on the decay of muons ("Neutrino Factories", NF [13, 45]) or of beta-unstable ions ("Beta Beams" [19]) have been proposed. In both cases, the initial flavor exploited to study subdominant transitions is ν_e or $\overline{\nu}_e$ oscillating into ν_μ and $\overline{\nu}_\mu$, respectively[1]. In particular, in the Beta Beam, the experimentalist benefits of a nearly ideal knowledge of the flavor and spectrum of the neutrinos and, contrary to the Neutrino Factory, of the presence of just one neutrino flavor in the initial state (ν_e for β^+ and $\overline{\nu}_e$ for β^- unstable isotopes). However, the choice of available isotopes is rather narrow: the ions employed in a Beta Beam must be produced at high yields to reach sizable neutrino fluxes; ions cannot decay too early to allow for acceleration and injection in a dedicated storage ring (from here on called the "decay ring") equipped with straight sections that point toward the far detector; on the other hand, ions cannot decay too slow so to have a sizable neutrino flux at the far detector in a short time, or equivalently, to avoid that partially filled bunches of ions remain in the decay ring for too many turns complicating the injection of new bunches. Besides the difficulties in producing, accelerating and storing unstable ions, the Beta Beam technology suffers from an important drawback with respect to the Neutrino Factory. Both facilities envisage a front-end stage where muons or ions are produced and manipulated to fit the acceptance of a chain of boosters. The boosters increase progressively the energy of the particles and at the exit of the last element of the chain (terminal booster) the muons or the ions are injected and stacked into the decay ring. Now, for any realistic terminal booster, the NF will produce neutrinos with much larger energy than the Beta Beam. A further problem of the Beta Beams facilities is that, due to the Z/A ratio of the injected ions, much longer rings are needed in order to maintain an intense flux aiming at the far detector with respect to Neutrino Factories. The typical size of a racetrack NF ring is $L_{ring} \sim 1500$ m, compared to $L_{ring} \sim 7000$ m for $\gamma = 100$ Beta Beams storing ^{6}He and ^{18}Ne ions [19].

With these problems in mind, the original Beta Beam design was conceived to leverage at most the CERN accelerator complex and profit of the high isotope production yield reachable by ISOL techniques [46]: in this framework the natural terminal booster was the SPS, which can accelerate ions up to a maximum Lorentz γ of $\simeq 450 \cdot Z/A$, while the choice of the ions came down to ^{6}He and ^{18}Ne with Q-values of 3.51 and 3.41 MeV, respectively. As a consequence, the mean energy of the neutrinos ($\simeq \gamma Q$) does not exceed $\sim$0.5 GeV ($\sim$0.9 GeV) for ^{6}He (^{18}Ne) [27]. Massive, low-density detectors are needed to overcome the smallness of the cross section and the dominance of quasi-elastic scattering at these energies, so that the detectors at the far location require, like for Superbeams, the construction of large underground infrastructures, as the proposed extension of the Modane Laboratories up to 10^6 m^3 [47]. As noted first in Ref. [26], working at larger mean energy has a remarkable impact on the physics performance provided that ion production and decay rate can be kept at the same level as for the previous options. Employing neutrinos in the multi-GeV range exhibits an additional advantage: the oscillation signal (ν_μ CC events in the bulk of unoscillated ν_e NC and CC interactions) can be observed and effectively separated from the background in high

[1] On the contrary, intense neutrino beams based on π decays ("Superbeams") study the T-conjugate of the transition measured by the Neutrino Factories or the Beta Beams, i.e. $\nu_\mu \to \nu_e$ and $\overline{\nu}_\mu \to \overline{\nu}_e$.

density, moderate granularity detectors [30] hosted in underground halls much smaller than the ones envisaged for Superbeams, such as the Gran Sasso underground laboratory (LNGS).

One option to achieve a larger mean neutrino energy is to use a new terminal booster of larger rigidity, as the proposed SPS+ [48], that would permit to increase the maximum γ. A higher γ would be ideal[2] since larger γ are beneficial for the flux at the far detector. Notice, however, that the decay rate at the storage ring decreases due to the larger ion lifetime in the lab frame ($\gamma\tau$). In fact, the neutrino flux per solid angle in a far detector located at a baseline L from the source, on-axis with respect to the boost direction of the parent ion is [26]:

$$\left.\frac{d\Phi}{dSdy}\right|_{\theta\simeq 0} \simeq \frac{N_\beta}{\pi L^2}\frac{\gamma^2}{g(y_e)} y^2(1-y)\sqrt{(1-y)^2-y_e^2}, \tag{1}$$

where $0 \leq y = \frac{E}{2\gamma E_0} \leq 1 - y_e$, $y_e = m_e/E_0$ and

$$g(y_e) \equiv \frac{1}{60}\left\{\sqrt{1-y_e^2}(2-9y_e^2-8y_e^4) + 15y_e^4 \log\left[\frac{y_e}{1-\sqrt{1-y_e^2}}\right]\right\}. \tag{2}$$

In this formula $E_0 = Q + m_e$ is the electron end-point energy in the center-of-mass frame of the β-decay, m_e the electron mass, E the energy of the final state neutrino in the laboratory frame and N_β the total number of useful ion decays per year. At larger γ, the mean neutrino energy increase as γQ and the flux as γ^2. To evaluate the actual advantage with respect to the SPS-based option, we consider the number of events at the far location for setups where the detector is always positioned at the peak of the oscillation maximum ($|\Delta m^2_{23}|L/4E = \pi/2$). For a given number of decays per year N_β in the decay ring, the events at the far location are proportional to the convolution of the flux ($\phi \sim \gamma^2/L^2$), of the cross section[3] ($\sigma \sim E \sim Q\gamma$) and of the oscillation probability, times N_β. If the facility is operated at the first maximum of the oscillation probability, then $|\Delta m^2|L/4E = \pi/2$ and, therefore, $L \sim Q\gamma$. As a result, the number of events is proportional to

$$N \simeq \frac{N_\beta\ \gamma}{Q} \tag{3}$$

An increase of γ is therefore beneficial, provided that the ion decay rate N_β does not drop faster than γ^{-1} [29, 49]: this is possible in spite of the relativistic $\gamma\tau$ increase of the lifetime because, in general, a higher γ allows for a larger number of ions to be stacked in the decay ring, since the length of a high-γ ion bunch is reduced by a factor γ due to Lorentz contraction and thus the occupancy of the ring can be maintained fixed. In summary, it can be shown that high-γ Beta Beam are outstanding tools to improve our knowledge of leptonic mixing, but they must still overcome two important technical challenges:

- they need a terminal booster with larger rigidity than the SPS and appropriate power to stand the yield obtained at the ion production front-end;
- they need a decay ring whose curved sections have a rigidity comparable or larger than of one of the terminal booster (i.e., they need longer rings with respect to low-γ Beta Beam).

On the other hand, none of these challenges have to be faced if the energy increase of the neutrino is achieved employing isotopes with larger Q-values: for example, the SPS can still be used as a booster; the ring needed to store high-Q ions can be a bit shorter than the one proposed for low-Q ions (or

[2]For a discussion of this option specifically focused on LNGS, see Ref. [30].

[3]In fact, the energy of the SPS-based Beta Beam is so small that the linear approximation for the cross section rise is inappropriate and the advantage of the increase of γ is even larger than what accounted here [34].

ions with a moderately higher γ can be stored in the same ring). Until 2006, however, Beta Beam with ions different from ^{6}He and ^{18}Ne was not considered, one of the motivation being the scaling of the number of events at the first peak shown in Eq. 3 (see, however, Ref. [50]).

In Ref. [51], the production using ISOL techniques and the acceleration stage using the PS and SPS have been reviewed. A new technique to produce low-Z, high-Q ions, however, was proposed in 2006 by C. Rubbia [32] and Y. Mori [52] and specifically adapted to high-Q Beta Beam in Refs. [32, 33] through the production of ^{8}Li and ^{8}B as $\overline{\nu}_e$ and ν_e sources, respectively. This technique is a new application of ionization cooling [53] particularly suited for strongly interacting beams. For the case of the high-Q Beta Beam, intense beams of ^{7}Li (^{6}Li) are stacked into a small storage ring containing a deuterium (^{3}He) target. Ionization losses in the target "cool" transverse betatron oscillations and the mean energy loss along the longitudinal direction can by compensated by means of RF cavities. The longitudinal motion of the beam, however, is intrinsically unstable because faster particles ionize less than average while slower ones ionize more and, hence, the momentum spread increase exponentially with time. Such instability is cured locating the target in a point of the ring that exhibits a chromatic dispersion, i.e. a point where particles are displaced from the nominal orbit position proportionally to their momentum spread. If the thickness of the target grows linearly with the radius of the orbit, faster particles (orbiting at larger radii) will cross a thicker area and, therefore will loss more energy by ionization. Similarly, slower particles orbit at lower radii and lose less energy than average due to the reduced thickness of the target. A wedge-shaped target, therefore, can restore stability in the longitudinal motion. This technique allows for the production of ^{8}Li through $^7\mathrm{Li} + \mathrm{D} \to {}^8\mathrm{Li} + \mathrm{p}$ and ^{8}B through $^6\mathrm{Li} + {}^3\mathrm{He} \to {}^8\mathrm{B} + \mathrm{n}$ by inelastic collisions of the stacked ions onto the shaped target.

Either using the ionization cooling technique or standard ISOL methods, a significant ^{8}Li flux can be produced (for ISOL techniques, the production rate of ^{8}Li is 100 times larger than for ^{6}He [54]). The ionization cooling technique should guarantee a similar production rate for ^{8}B. In this case, however, the main problem resides in the extraction and recollection of ^{8}B ions: they react with many elements typically used in targets and ion sources and are therefore difficult to manipulate. Eventually, it must be reminded that the ^{8}B β-decay spectrum is affected by several systematics errors that must be tamed before using it for a precision experiment (see Ref. [55]).

The issue of ion production and extraction from the storage ring [21], of the effectiveness of cooling [56] and of the yields actually sustainable by the SPS are at the focus of current accelerator research in Beta Beam. It must be shown, in fact, which are the maximal yields that can be effectively produced and extracted from the source area for a given low-Q or high-Q ion, and that the rest of the booster chain can sustain these yields.

In the framework of the EUROν Design Study [21] the proposed Beta Beam (see Fig. 1) exploits the CERN accelerator complex as it evolves in the forthcoming years to cope with the needs of the LHC. In particular, the Beta Beam facility does not require the construction of a new terminal booster, neither as a dedicated machine nor as an ancillary facility shared with the LHC (as for the case of the SPS+). The only assumption made on the evolution of the CERN complex is the replacement of the Proton Synchrotron with a new machine (PS2 [57]) injecting protons at an energy of 50 GeV into the SPS. Such replacement is presently envisioned to grant the reliability of the LHC injection complex and for the luminosity upgrade of the LHC itself.

3 A facility exploiting at most existing infrastructures

The facility that we consider in this paper does not differ from the baseline EUROν [21, 44] design, but for a high density far detector located in a pre-existing hall at LNGS. The rationale behind this choice can be described starting from Fig. 2. The dashed (black) line shows the neutrino energy spectrum (in a.u.) for ^{8}B at $\gamma = 100$ as a function of the neutrino energy (in GeV). In the same plot, the continuous black line represents the ratio between the quasi-elastic and total cross section

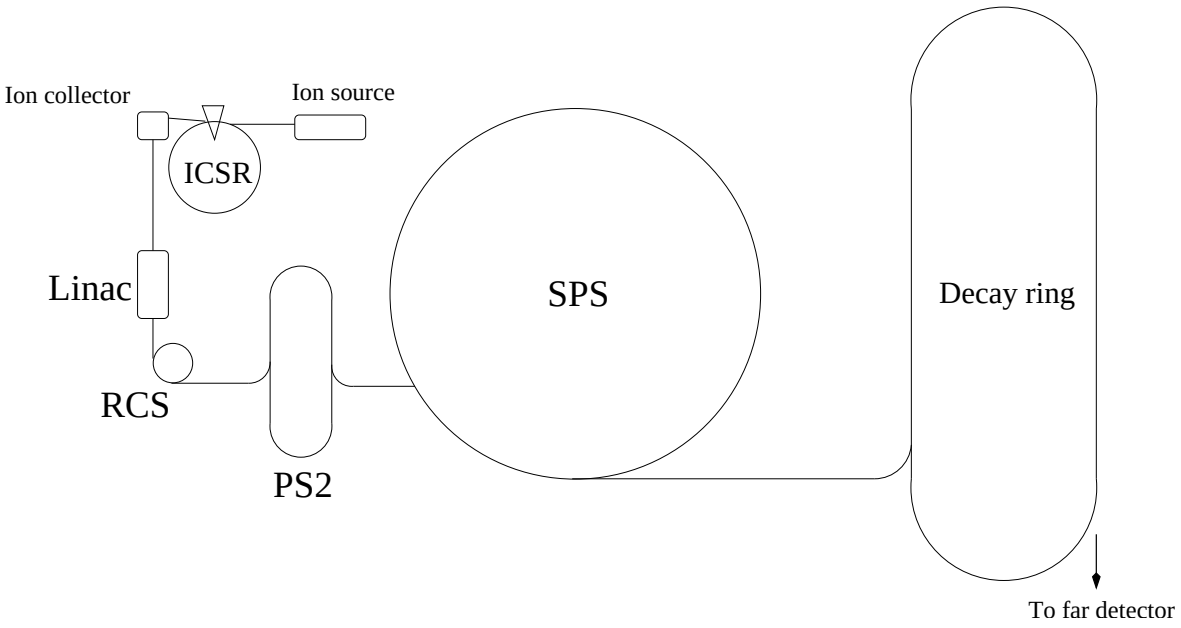

Figure 1: The machine complex for a high-Q Beta Beam in the EUROν scenario. The front-end ion (^{7}Li and ^{6}Li) source ("Ion source") is a 20 MeV linac injecting the isotopes into the ionization cooling storage ring ("ICSR"). Ions produced in the ring by inelastic interaction with the wedged target are collected, separated ("Ion collector") and sent toward a first stage booster ("Linac"). A dedicated Rapid Cycling Synchrotron (RCS) and the PS2 further accelerate the ions before injection into the terminal booster (the existing CERN-SPS). Eventually, ions are injected into the decay ring and stacked. Ions decaying in the straight session of the ring produce ν_e or $\overline{\nu}_e$ pointing toward the far detector.

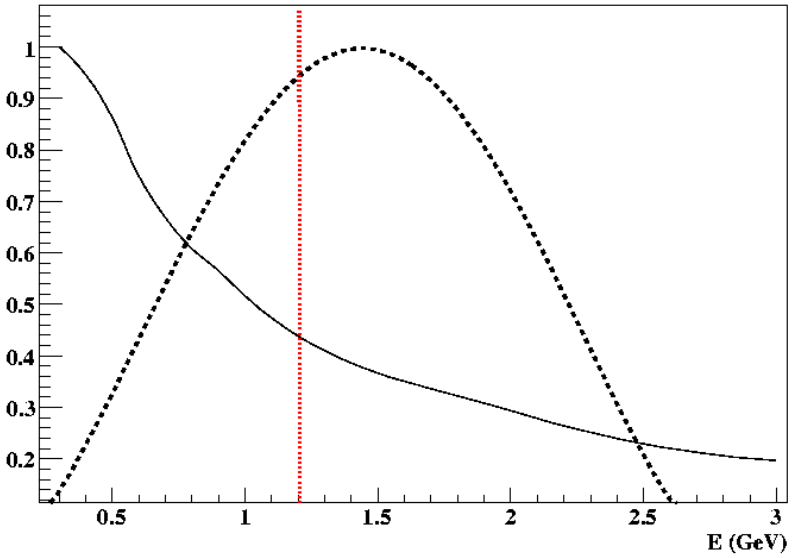

Figure 2: Dashed black line: the flux of neutrinos at the far detector from the decay of ^{8}B boosted at $\gamma = 100$ (in a.u.) versus the neutrino energy (in GeV). The continuous black like represents the ratio between quasi-elastic and total cross section in ν_μ CC interactions. The vertical dotted (red) line shows the muon energy needed to reach a range in iron larger than 4.6 interaction lengths, corresponding to a residual contamination of punch-through non-interacting pions lower than 10^{-2}.

in ν_μ CC interactions [58]: at the energy of the neutrinos from high-Q ions boosted by the SPS, such ratio is heavily suppressed, favoring detectors that are capable to identify not only quasi-elastic topologies (e.g. the "single ring" events in water Cherenkov detectors) but also deep-inelastic or resonant ν_μ interactions (segmented liquid scintillators, liquid argon TPC's or iron calorimeters). In particular, when the mean muon range exceeds the pion interaction length, high density detectors (iron calorimeters) can be employed to separate the ν_μ CC signal from the bulk background of ν_e NC and ν_e CC since hadrons are effectively filtered by the passive material. The vertical dotted (red) line in Fig. 2 shows the energy needed by a muon to reach a range in iron sufficient to filter pions at the 10^{-2} level, i.e. the energy range where signal efficiency for iron calorimeters is expected to be large (see Sec. 4). As a consequence the EUROν design option is properly suited for the exploitation of detector technologies based on high density absorbers even with the present SPS employed as a terminal booster.

Once fixed the detector technology, we must determine the achievable neutrino flux. This is the most relevant information needed to evaluate the physics performance of this facility, and it depends on the amount of "useful decays per year" of the stored ions, i.e. the amount of ions that decay in the straight section of the decay ring (see Fig. 1) pointing to the far detector. This, in turn, depends on the size, geometry and lattice design of the decay ring (the optimization of which is one of the goals of the EUROν accelerator R&D) and on the number of ions that can be stored simultaneously into the ring in one year, N_{ions}.

We first discuss the impact of the ring geometry on the neutrino flux. Independently of the ions chosen, cost and practical considerations constrain the size of the ring up to about the size of the SPS, $L_{ring} = 6880$ m. A decay ring made of relatively small curved sections (with radius of the curved section $R \sim 300$ m) followed by long straight sections ($L_{straight} = 2500$ m) pointing toward the

detector was considered as a natural geometry for a single far detector, while for multiple baselines, a triangular geometry might be more appropriate [37] (see, however, Ref. [43] and the ISS Physics Final Report, Ref. [15]). Decays that provide useful neutrinos are those occurring in the straight section(s) where neutrinos fly in the direction of the detector(s). The useful fraction of decays, called the "livetime" $l = L_{straight}/L_{ring}$ (where L_{ring} is the total length of the ring), depends on the geometry of the ring: for a racetrack geometry, $L_{ring} = 2\pi R + 2L_{straight}$. Once the livetime is eventually fixed, then the neutrino flux is given by $N_\beta = l \times N_{ions}$. In the EURISOL option the livetime was $\sim 36\%$ for $L_{ring} = 6880$ m. For fixed straight sections, the livetime depends on the minimum R that can be achieved, which in turn depends on the gyroradius ρ [59] of the ion

$$\rho = p/|Z|B = \gamma\beta A m_p/|Z|B\,, \tag{4}$$

B being the maximum bending field, m_p the proton rest mass and Z, A the atomic number and weight of the stacked isotope. Since the A/Z ratio of ^{18}Ne and ^{8}B (1.8 versus 1.6) and of ^{6}He and ^{8}Li (3.0 versus 2.7) are very similar, both pair of ions can circulate in the same ring geometry, with similar livetime[4]. Motivated by these considerations, in the following we will maintain the same livetimes as for the EURISOL option, $l = 0.36$.

The number of stored ions N_{ions} depends on a number of factors related to the production and manipulation of the beam, on which we can say little (the study of it is part of the EURISOL project goal for ^{6}He and ^{18}Ne and of the EUROν project for ^{8}Li and ^{8}B). Once the maximum number of ions that can be collected and boosted at the desired energy is known, however, they must still be properly distributed in short bunches inside the storage ring in order to use time-correlation to reduce the atmospheric neutrino background at the far detector. The required duty cycle is very demanding: previous analysis showed that for ^{6}He and ^{18}Ne ions boosted at $\gamma \sim 100$ the decaying ions must be accumulated in very small bunches occupying just a very small fraction of the storage ring. It has been shown in Refs. [60, 44] that a 10^{-3} suppression of the atmospheric background (i.e., a 10^{-3} duty cycle) is needed in order to achieve a good sensitivity to physics observables. This puts a strong constraint on the manipulation of the beam that can result in a reduction of the ultimate neutrino flux (being the storage ring not used at its maximum capacity). In other words, although a given number N of ions can be produced and accelerated at the desired boost, only a fraction of them can be actually injected into the storage ring if we want to attain the required atmospheric background suppression.

It has been suggested in several papers that increasing the neutrino energy allow for less demanding duty cycles (see, for example, Refs. [26, 27] and [37]), that in turn permit to store more ions into the storage ring (see Ref. [61]). The net result is that either a larger neutrino flux aims at the far detector or, alternatively, a lesser technological effort would be needed to achieve the desired flux. Unfortunately, in Ref. [44] it was shown that it is not possible to relax the duty cycle too much for ^{8}Li and ^{8}B ions boosted at $\gamma = 100$ with respect to ^{6}He and ^{18}Ne boosted at the same γ without losing sensitivity to the physics observables, assuming that in both setups an $O(1)$ Mton class water Čerenkov is used as far detector In fact, most considerations hold for the present setup, as well. We will assume in the rest of the paper a suppression factor in the ballpark of 10^{-3} , therefore neglecting background from off-time atmospheric neutrinos.

The nominal fluxes proposed in the EURISOL project for ^{18}Ne and ^{6}He are 1.1×10^{18} ^{18}Ne and 2.9×10^{18} useful decays per year, respectively. Preliminary studies show that the nominal flux is at hand for ^{6}He ions (the estimations actually yield a flux somewhat larger, of 3.18×10^{18} useful decays per year). In the case of ^{18}Ne, on the other hand, the production of an intense flux is much more challenging and the present estimates fall two orders of magnitude short of the mark, yielding a flux of 4.6×10^{16} useful decays per year (see Ref. [62]). As discussed in Sec. 2, significantly larger fluxes

[4]Notice that a reduction of the curved sections of the ring, with a smaller ring size (and, correspondingly, a reduced cost) and an increased livetime could be achieved employing superconducting magnets similar to the ones currently installed for the LHC (8.3 T) .

are expected from the use of ionization cooling for high-Q isotopes (although it is not clear if ^{8}B ions can be recollected in huge numbers). For this reason, in the rest of the paper, we will study the performance of our setup as a function of the achievable neutrino and antineutrino flux, F and $\bar{F}$, with respect to a nominal flux F_0, for $F_0 = 3 \times 10^{18}$ useful decays per year for both ^{8}B and ^{8}Li.

4 Detector simulation

The description of a massive iron detector capable to exploit a high-energy Beta Beam and the efficiencies and background calculations, have been detailed in Ref. [30]. Here, the detector consisted of a sandwich of 4 cm iron slabs interleaved with glass RPC's to reach an overall mass of 40 kton. The RPC are housed in a 2 cm gap while the active element is a 2 mm gas-filled gap, whose signal is digitally read-out by 2×2 cm^2 pads. A full GEANT3 [63] simulation of this geometry has been implemented along the lines discussed in Ref. [64], including a coarse description of the RPC materials and an approximate description of the digitization process. As detailed in Ref. [64], the accuracy of this simulation was validated by comparing its predictions to existing data collected with a small prototype exposed to a pion beam of energy from 2 GeV to 10 GeV [65].

The variables that are used for event classification are purely inclusive: the total number of hits and event length expressed in terms of number of crossed iron layers. Since in the high-Q configuration considered in Sec. 3 the mean neutrino and antineutrino energies are both 1.5 GeV, we employ the same selection both for ν_μ CC and $\bar{\nu}_\mu$ CC events: an interaction is classified as a ν_μ ($\bar{\nu}_\mu$) CC if both the event length and the total number of hits in the detector are larger than 12. The efficiency for identifying a neutrino CC interaction averaged out over the whole spectrum is $\sim 60\%$. Conversely, the probability for the background to be identified as a CC-like event is slightly less than 1%. Efficiencies and background contaminations as a function of the neutrino energy are shown in Fig. 3 (see also Ref. [30]).

It is worth noting that for larger energies the performance of the detector is comparable with the one proposed for the Neutrino Factory, the mean neutrino energy at NF being much larger (~ 30 GeV) than for a high-Q Beta Beam. The main difference is due to the fact that here the magnetization of the iron is not mandatory since Beta Beams are pure sources of ν_e and the identification of the muon charge at the final state is immaterial. Charge identification is only beneficial to reduce the background of punch-through pions while for the NF it is essential to veto "right sign" events originating from $\bar{\nu}_\mu$ produced at the source [16, 45]. The same detector considered here can serve as a far detector for a Neutrino Factory when the iron is magnetized by magneto-motive forces comparable to the one envisaged for MIND [66, 67].

Once more, it is interesting to assess the configuration that exploits at most existing infrastructures, with emphasis on the opportunities offered by the LNGS experimental Halls. In [30] we considered a setup inspired by the MONOLITH proposal [68]. MONOLITH, in its original design, would have been installed in the position presently occupied by the OPERA experiment [69]. Such allocation in the Hall C of LNGS limited the fiducial mass up to 34 kton. In fact, the Hall C is much larger: it includes the Borexino experiment [70], the test facility CTF between Borexino and OPERA and the pseudocumene storage tanks positioned just in front of OPERA. Therefore, the maximum longitudinal size that can be allocated is 90 m, assuming the Beta Beam far detector to be the only user of the Hall. To make the installation feasible, the horizontal size cannot exceed 14.5 m. Hence, the maximum mass conceivable in Hall C is $\sim$100 kton. As noted in the framework of the NF [16], an investment aimed at increasing the mass of the detector offers a better cost/benefit ratio with respect to a prolongation of the data taking of the NF or the Beta Beam. Such benefit is lost if a dedicated underground hall must be built on purpose to extend the detector inside a deep underground site.

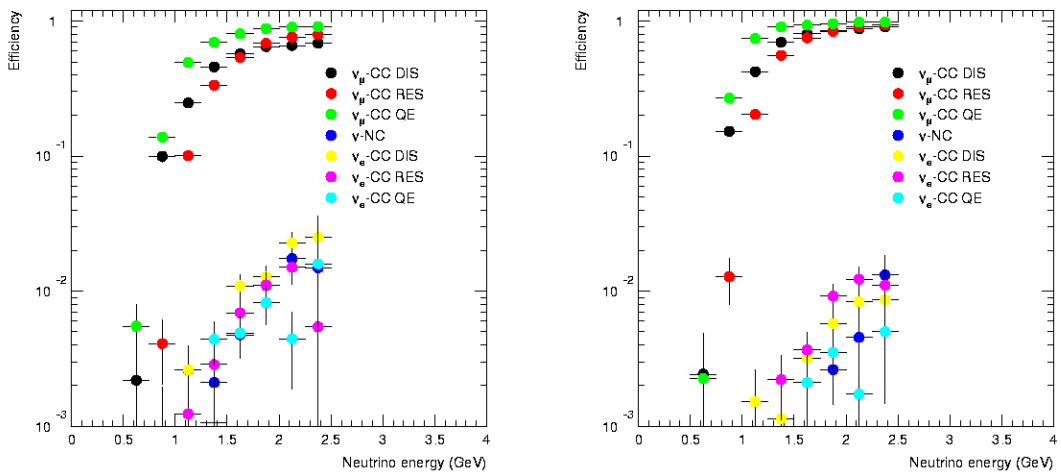

Figure 3: Efficiencies for the signal (ν_μ and $\bar{\nu}_\mu$ charged-current interactions) to be identified as CC-like event and for the background (ν_e and $\bar{\nu}_e$ interactions, and ν_μ and $\bar{\nu}_\mu$ neutral-current interactions) to be mis-identified as a CC-like events.

5 Results

In this section we will study the physics performance of the proposed setup in terms of two observables, defined as follows:

the CP discovery potential: for a given point in the parameter space, we will say that CP violation can be discovered if we can rule out the no CP violation hypothesis ($\delta = 0°$ and $180°$) at 3σ 1 d.o.f., after marginalizing over all the remaining parameters for both possible hierarchies.

the sgn(Δm^2_{23}) reach: this is defined as the region of the $(\sin^2 2\theta_{13}, \delta)$ plane for which the wrong hierarchy can be eliminated at 3σ. Below this value of $\sin^2(2\theta_{13})$, the predictions for the wrong hierarchy cannot be distinguished from the data corresponding to the right hierarchy, at a statistical significance of 3σ.

Notice that, in both cases, results will be presented as a function of $\sin^2(2\theta_{13})$. However, as we have already explained in Sec. 3, the physics reach of the setup strongly depends on the achievable fluxes. Therefore, in the next subsections results will also be presented as a function of the flux ratios F/F_0 and $\bar{F}/F_0$, being $F_0 = 3 \times 10^{18}$ useful decays per year. A 100 kton detector mass is assumed together with a data taking duration of 5 years in neutrino and 5 year in antineutrino mode.

5.1 Sensitivity to the CP-violating phase

In Fig. 4, the discovery potential is presented as a function of the neutrino and antineutrino fluxes F and $\bar{F}$ with respect to F_0, for several representative values of δ and θ_{13}. For the points in the region below and to the left of each line, CP violation cannot be established at 3σ 1 d.o.f. after marginalizing over the rest of parameters. The diagonal dashed black line represents the points where the same neutrino and antineutrino flux ratios are considered, $F = \bar{F}$. Notice that, if we restrict both fluxes to the reference value F_0 (marked as a red circle in the plot), then CP violation cannot be determined

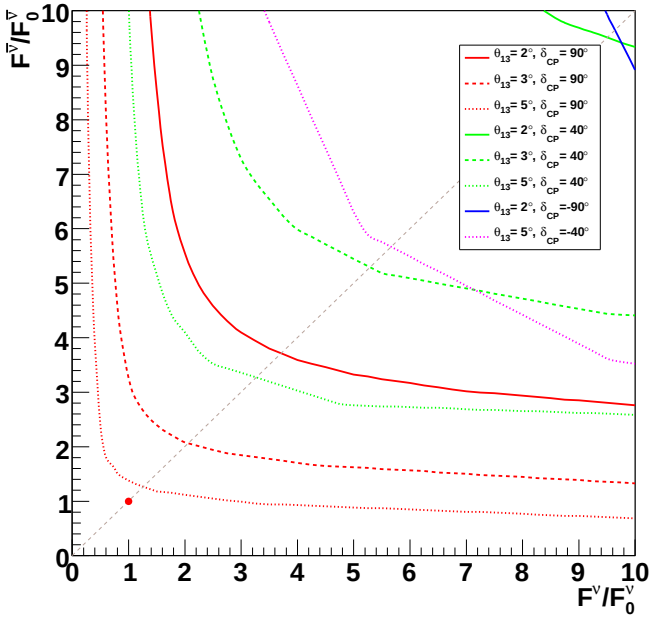

Figure 4: CP discovery potential as a function of both neutrino and antineutrino fluxes (F and $\bar{F}$, respectively) with respect to the nominal flux F_0, for several input values of δ and θ_{13}, shown in the legend. The dashed black line determines the points were the same neutrino and antineutrino fluxes are considered, $F = \bar{F}$. The red circle shows the point where both fluxes correspond to the reference value, $F_0 = 3 \times 10^{18}$ useful ion decays per year. Lines of the same color correspond to the same δ values, while lines of the same type (continuous, dotted, dashed) correspond to the same values of θ_{13}. For the points in the region above and to the right of each line, CP violation can be established at 3σ 1 d.o.f. after marginalizing over the rest of parameters, at least for one point in the parameter space.

for any pair of the (δ,θ_{13}) values we have considered. Even for maximal CP violation ($\delta = \pm 90°$) and increasing θ_{13} up to 5°, a 40% increase of the flux for both polarities is needed in order to establish CP violation at least for one point in the parameter space. On the other hand, if we fix the neutrino flux ratio at $F/F_0 = 1$, maximal CP violation can be established at 3σ for $\theta_{13} = 3°(5°)$ if we manage to achieve an antineutrino flux ratio $\bar{F}/F_0 = 3(1.4)$. It is also important to notice that, for negative values of δ only two of the lines are visible in the plot, corresponding to the input values ($\delta = -90°$, $\theta_{13} = 5°$) and ($\delta = -40°$, $\theta_{13} = 2°$), but no line is present in the plot for $\theta_{13} = 3°$ and $\delta < 0$. This is due to the so-called "π-transit" effect [71]: matter effects mimic true CP violation and, for this particular value of θ_{13}, when $\delta < 0$ the so-called "sign clones"[5] move from the true CP-violating values to CP-conserving ones. As a consequence, in this particular region of the parameter space CP violation cannot be established even if it is maximal[6].

This effect can also be appreciated in Fig. 5, where the CP discovery potential is plotted as a function of the neutrino flux ratio, F/F_0, for $\theta_{13} = 2°$, 3°, and 5°, keeping the antineutrino flux ratio fixed at $\bar{F}/F_0 = 10$. For the points located to the left of each line in the plot, CP violation cannot be established at 3σ CL after marginalization over the rest of parameters. It can also be seen here that

[5]Degenerate minima of the χ^2 corresponding to a wrong assignment of the neutrino mass hierarchy and to a different pair (θ_{13}, δ), see Refs. [72, 73, 74].

[6]This effect depends strongly on the amount of matter effect observed at the considered setup. For the Neutrino Factory, where it was discussed first, the π-transit occurs for $\sin^2 2\theta_{13} \sim 10^{-3} (\theta_{13} \sim 1°)$.

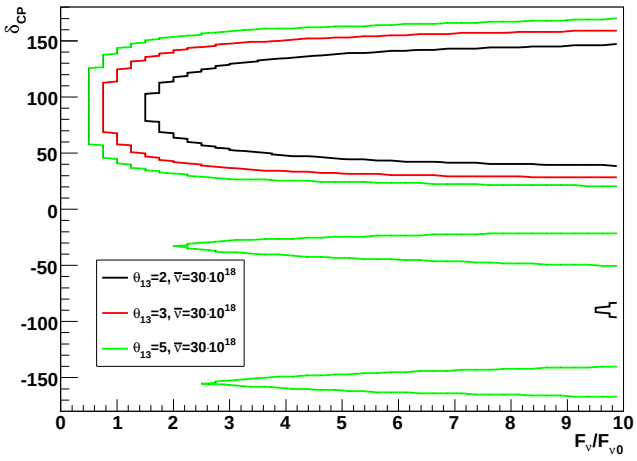

Figure 5: CP discovery potential as a function of the neutrino flux F and δ, for several values of θ_{13}, and an antineutrino flux ratio $\bar{F}/F_0 = 10$. For the points in the region to the left of each line, CP violation cannot be established at 3σ 1 d.o.f. after marginalizing over the rest of parameters.

the CP discovery potential is quite poor in the $\delta < 0$ region: for $\theta_{13} = 2°$, we are only sensitive to CP violation if it is maximal for extremely high values of the neutrino flux ratio, while for the $\theta_{13} = 5°$ case two narrow bands appear around $\delta = -40°$ and $-150°$. Again, when $\theta_{13} = 3°$, CP violation cannot be established for any negative value of δ.

Finally, we show in Fig. 6 the CP discovery potential as a function of θ_{13} and δ, for several values of the neutrino and antineutrino flux ratios. Notice the vertical dotted lines, which indicate, from left to right in the plot, the values of $\sin^2(2\theta_{13})$ corresponding to $\theta_{13} = 1°$, $2°$ and $3°$, respectively. We see again a strong lack of sensitivity around $\sin^2(2\theta_{13}) \sim 10^{-2}$, which corresponds to $\theta_{13} \sim 3°$, due to the π-transit phenomenon. It can also be seen how, for smaller values of θ_{13}, we recover some sensitivity to CP violation.

Regarding the statistical dependence of the setup, a strong improvement takes place when the antineutrino flux is increased from $F_0 \to 4F_0$, even though we keep the neutrino flux fixed at F_0. However, once we have reached this point, we get practically no improvement at all if we keep increasing the antineutrino flux unless the neutrino flux is also enhanced. This can be seen from the comparison of the red and green lines: we have increased the antineutrino flux another factor 2.5 (up to $10F_0$), but the CP discovery potential improvement is quite mild. This is due to the fact that, in order to achieve sensitivity to the CP-violating phase, a comparison between the neutrino and antineutrino oscillated events is mandatory: even if we continue increasing the antineutrino flux the CP discovery potential will not increase unless we have enough neutrino events to compare with. This is precisely what happens when we compare the green and blue lines in the plot: the improvement is remarkable in this case, though only the neutrino flux has been enhanced, because now all the antineutrino events are useful.

5.2 Sensitivity to the neutrino mass hierarchy

In Fig. 7, the sensitivity to the neutrino mass hierarchy is presented as a function of the neutrino and antineutrino fluxes F and $\bar{F}$ with respect to F_0, for several representative values of δ and θ_{13}. The left panel refers to the normal hierarchy, the right panel to the inverted one. For the points in

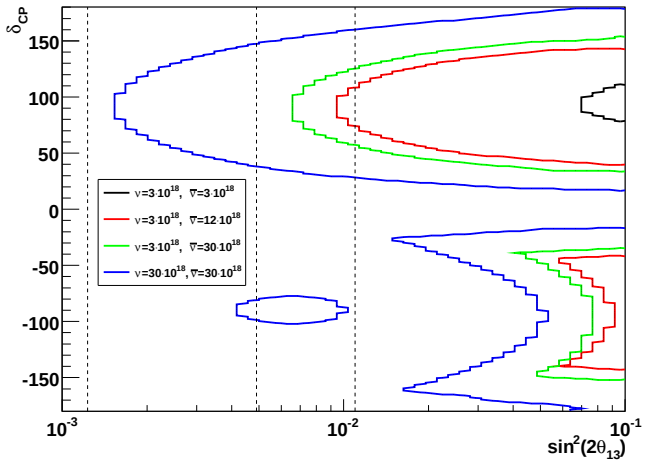

Figure 6: CP discovery potential as a function of $\sin^2(2\theta_{13})$ and δ, for several values of both neutrino and antineutrino flux ratios, as indicated in the legend. The dashed vertical lines show, from left to right, the values of $\sin^2(2\theta_{13})$ corresponding to $\theta_{13} = 1°$, $2°$ and $3°$, respectively. For the points in the region to the left of each curve, CP violation cannot be established at 3σ 1 d.o.f. after marginalizing over the rest of parameters.

the region above and to the right of each line, a given hierarchy can be established at 3σ 1 d.o.f. after marginalizing over the rest of parameters, for the particular choice of input parameters. The diagonal dashed black line represents the points where the same neutrino and antineutrino flux ratios are considered, $F = \bar{F}$. Notice that, if we restrict both fluxes to the reference value F_0 (marked as a red circle in the plot), then the hierarchy cannot be determined for any pair of the (δ,θ_{13}) values we have considered. Also in this case, as it was for the CP violation discovery potential, we need a 40% increase of the flux for both polarities in order to establish a given hierarchy at least for the largest considered θ_{13} value, $\theta_{13} = 5°$. As we have said, neutrino fluxes are unlikely to be much higher than the reference value. However, if we fix the neutrino flux ratio at $F/F_0 = 1$, with a 50% increase of the antineutrino flux we become sensitive to the hierarchy for this particular point in the parameter space, $\theta_{13} = 5°$, $\delta = +90°$ or $-90°$ (for normal or inverted hierarchy, respectively). For smaller θ_{13}, we need a neutrino flux $F = 2F_0$, at least (if, at the same time, we manage that the antineutrino flux is increased to $\bar{F} \sim 4F_0$).

As we have already mentioned in Sec. 5.1, as the baseline of the setup is relatively "short", matter effects turn out to be quite mild and therefore we are sensitive to the mass hierarchy only in a small region of the parameter space. The sensitivity to $\mathrm{sgn}(\Delta m^2_{23})$ is depicted in Fig. 8 (Fig. 9) as a function of $\sin^2(2\theta_{13})$ and δ, assuming normal (inverted) hierarchy, for several values of the neutrino and antineutrino fluxes. The vertical dashed lines indicate, from left to right, the values of $\sin^2(2\theta_{13})$ corresponding to $\theta_{13} = 1°$, $2°$ and $3°$, respectively. For the points located to the left of each curve, the correct hierarchy cannot be determined at a statistical significance of 3σ, after marginalization over the rest of parameters.

It can be seen that changing from normal to inverted hierarchy is practically equivalent to replacing $\delta \to -\delta$. In the limit of null matter effect, the sensitivity to $\mathrm{sgn}(\Delta m^2_{31})$ comes from the CP-violating term in the probability, which for normal hierarchy is maximal for neutrinos for positive values of δ, while for the inverted hierarchy it is maximal for antineutrinos and $\delta < 0$. The small asymmetry observed when we change from normal to inverted hierarchy and *viceversa* is due to a combination of two factors: on one side, matter effects enhance neutrino with respect to antineutrino events when

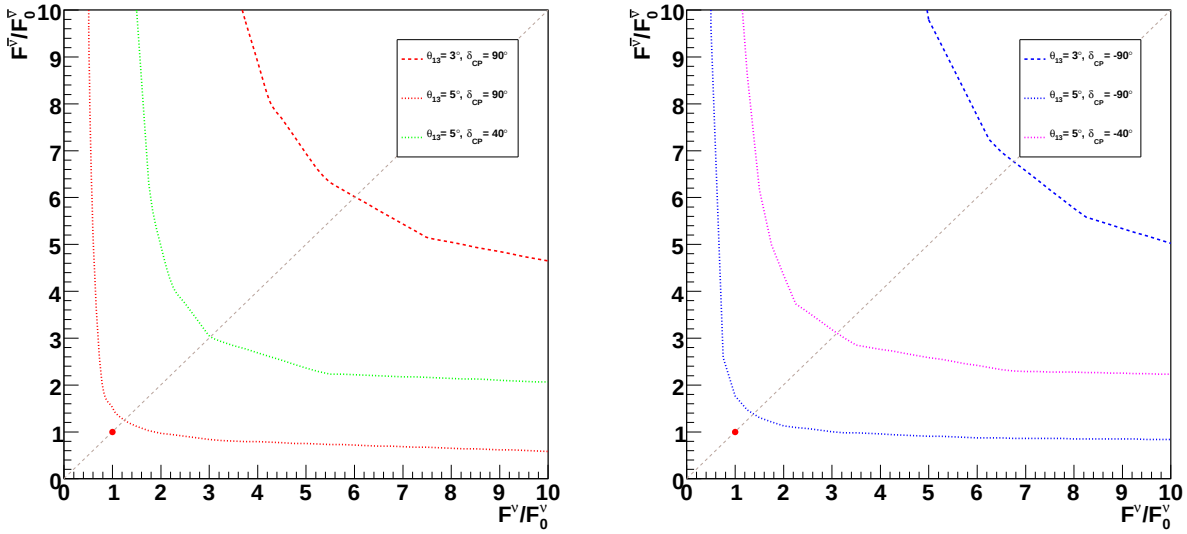

Figure 7: Sensitivity to the hierarchy as a function of both neutrino and antineutrino fluxes (F and $\bar{F}$, respectively) with respect to the nominal flux F_0, for several input values of δ and θ_{13}, shown in the legend. Left panel: normal hierarchy; right panel: inverted hierarchy. The dashed black line determines the points were the same neutrino and antineutrino fluxes are considered, $F = \bar{F}$. The red circle shows the point where both fluxes correspond to the reference value, $F_0 = 3 \times 10^{18}$ useful ion decays per year. Lines of the same color correspond to the same δ values. For the points in the region above and to the right of each line, a given hierarchy can be established at 3σ 1 d.o.f. after marginalizing over the rest of parameters, for the considered point in the parameter space.

the hierarchy is normal, while the opposite effect takes place if the hierarchy is inverted. On the other hand, as the antineutrino cross section is smaller, the lines with the same fluxes for both polarities are, in general, worse if we assume inverted hierarchy than if we assume normal hierarchy.

As noted in Ref. [31], a magnetized iron detector can fruitfully combine data from the Beta Beam and from atmospheric neutrinos to improve the sensitivity on the mass hierarchy [75]. For large values of θ_{13}, such combination can be of value for the present setup in the occurrence of normal (inverted) hierarchy and negative (positive) values of δ, i.e. in the region of null sensitivity of Fig. 8 and 9. The combination is depicted in Fig. 10 assuming $F = \bar{F} = 10F_0$. In particular, for $\delta = -90°$ atmospheric neutrinos bring the 3σ sign sensitivity of the setup down to $\sin^2 2\theta_{13} \simeq 3 \times 10^{-2}$.

6 Conclusions

Since its inceptions, Beta Beams have been conceived to exploit in an optimal manner existing facilities in order to establish CP violation in the leptonic sector. In this paper, we considered a setup that leverages at most present European infrastructures. It is based on the CERN-SPS accelerator, which is employed to boost high-Q ions toward the Hall C of the Gran Sasso Laboratories.

For a far detector of 100 kton mass, a β^+-emitters (^{8}B) flux of approximately 6×10^{18} useful decays per year[7] is needed to observe CP violation in a large fraction of the parameter space (60%) for any value of θ_{13} that gives a positive signal at T2K ($\theta_{13} \gtrsim 3°$). This sensitivity to δ is deteriorated

[7]This is about three times the flux proposed for ^{18}Ne, where $F_0 \sim 2 \times 10^{18}$.

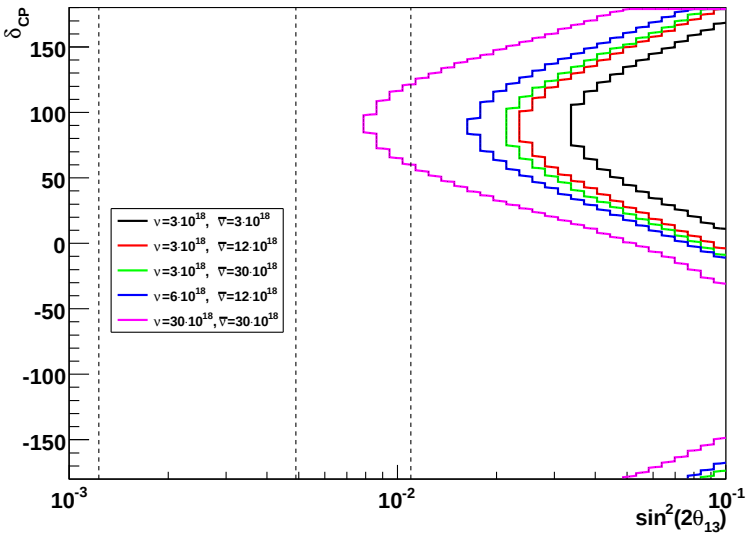

Figure 8: The $\mathrm{sgn}(\Delta m^2_{31})$ sensitivity as a function of $\sin^2(2\theta_{13})$ and δ for several values of both neutrino and antineutrino flux ratios, assuming normal hierarchy. The dashed vertical lines indicate, from left to right, the values of $\sin^2(2\theta_{13})$ corresponding to $\theta_{13} = 1°$, $2°$ and $3°$, respectively. For the points in the region to the left of each curve, the correct hierarchy cannot be established at 3σ 1 d.o.f. after marginalizing over the rest of parameters.

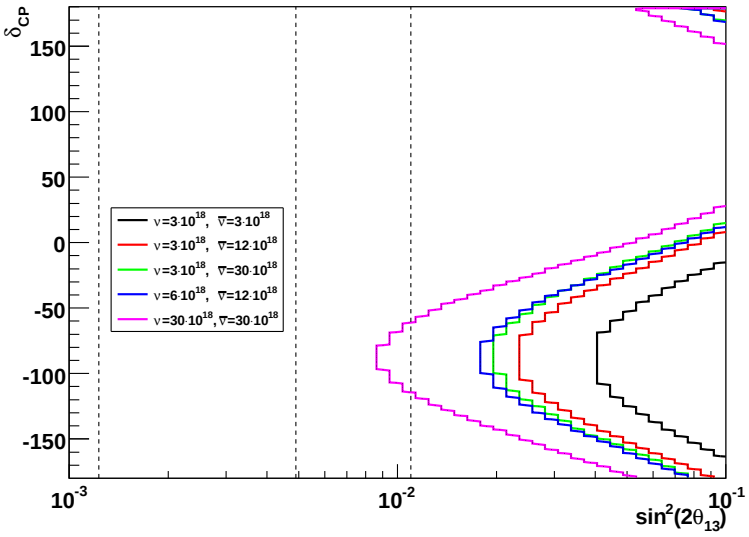

Figure 9: The $\mathrm{sgn}(\Delta m^2_{31})$ sensitivity as a function of $\sin^2(2\theta_{13})$ and δ for several values of both neutrino and antineutrino flux ratios, assuming inverted hierarchy. The dashed vertical lines indicate, from left to right, the values of $\sin^2(2\theta_{13})$ corresponding to $\theta_{13} = 1°$, $2°$ and $3°$, respectively. For the points in the region to the left of each curve, the correct hierarchy cannot be established at 3σ 1 d.o.f. after marginalizing over the rest of parameters.

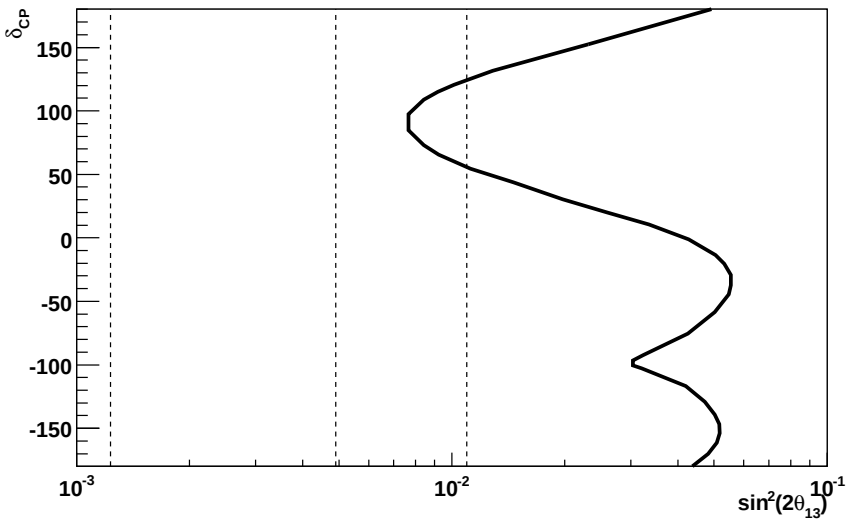

Figure 10: The $\mathrm{sgn}(\Delta m^2_{31})$ sensitivity as a function of $\sin^2(2\theta_{13})$ and δ for 3×10^{19} decays per year both for neutrinos and antineutrinos, assuming normal hierarchy. The dashed vertical lines indicate, from left to right, the values of $\sin^2(2\theta_{13})$ corresponding to $\theta_{13} = 1^\circ$, 2° and 3°, respectively. For the points in the region to the left of each curve, the correct hierarchy cannot be established at 3σ 1 d.o.f. after marginalizing over the rest of parameters.

for $\delta < 0$ due to the occurrence of the π-transit, as observed in other facilities. The ^{8}B flux must be accompanied by a ^8Li flux of $\sim 3 \times 10^{19}$ decays per year. Present studies on the ionization cooling technique or on ISOL-type targets indicate that such a large ^{8}Li flux could be feasible. Moreover, the former technique should produce β^+ and β^- emitters at a similar rate although ^{8}B ions interact stronger than ^{8}Li ions with materials in the target and in the recollection region. To achieve the fluxes above clearly represents the most challenging task for accelerator R&D but it is a viable option with respect to ^{18}Ne, where ISOL-type targets fall almost two orders of magnitude short of the goal.

In the same configuration, we find a non-negligible sensitivity to the neutrino mass hierarchy that extends up to $\theta_{13} \simeq 4^\circ$ for positive (negative) values of δ for normal (inverted) hierarchy. In the opposite parameter area, i.e. for negative (positive) values of δ and inverted (normal) hierarchy, the combination with atmospheric data collected during the Beta Beam run by the same magnetized detector further improves such sensitivity at large θ_{13} ($\simeq 6^\circ$). Combination of atmospheric data with Beta Beam–driven ones should also be able to solve part of the π-transit deterioration discussed above.

Acknowledgments

We wish to express our gratitude to T. Tabarelli de Fatis for many useful information on the simulation of magnetized iron detector. We gratefully acknowledge M. Mezzetto and F. Ronga for several interesting discussions. This work was supported by the European Union under the European Commission Framework Programme 07 Design Study "EUROν", project 212372. P.C. and A.D. acknowledge funding by the spanish ministry for Science and Innovation under the project FPA2009-09017 and the program "CUP" Consolider-Ingenio 2010, project CSD2008-0037; by the Comunidad Autónoma de Madrid through project HEPHACOS-CM (S2009ESP-1473). Eventually, P.C. acknowledges financial support from the Comunidad Autónoma de Madrid.

References

[1] Y. Itow *et al.* [The T2K Collaboration], arXiv:hep-ex/0106019.

[2] D. S. Ayres *et al.* [NOvA Collaboration], arXiv:hep-ex/0503053. See also `http://www-nova.fnal.gov`.

[3] F. Ardellier *et al.* [Double Chooz Collaboration], arXiv:hep-ex/0606025.

[4] X. Guo *et al.* [Daya-Bay Collaboration], arXiv:hep-ex/0701029.

[5] S. B. Kim [RENO Collaboration], AIP Conf. Proc. **981** (2008) 205 [J. Phys. Conf. Ser. **120** (2008) 052025].

[6] T. Schwetz, M. A. Tortola and J. W. F. Valle, New J. Phys. **10** (2008) 113011.

[7] M. Apollonio *et al.* [CHOOZ Collaboration], Eur. Phys. J. C **27** (2003) 331.

[8] F. Boehm *et al.*, Phys. Rev. D **64** (2001) 112001.

[9] M. C. Gonzalez-Garcia and M. Maltoni, Phys. Rept. **460** (2008) 1 [arXiv:0704.1800 [hep-ph]].

[10] A. B. Balantekin and D. Yilmaz, J. Phys. G **35** (2008) 075007; G. L. Fogli, E. Lisi, A. Marrone, A. Palazzo and A. M. Rotunno, Phys. Rev. Lett. **101** (2008) 141801; M. Maltoni and T. Schwetz, arXiv:0812.3161 [hep-ph].

[11] B. Aharmin *et al.*[SNO Collaboration], arXiv:0910.2984 [nucl-ex].

[12] M. Mezzetto, Proceedings of "Thirteen International Workshop on Neutrino Telescopes", Venezia, March 10-13, 2009, p. 421, arXiv:0905.2842 [hep-ph].

[13] A. De Rujula, M. B. Gavela and P. Hernandez, Nucl. Phys. B **547** (1999) 21.

[14] P. Huber, M. Lindner, T. Schwetz and W. Winter, JHEP **0911** (2009) 044.

[15] A. Bandyopadhyay *et al.* [ISS Physics Working Group], Rept. Prog. Phys. **72** (2009) 106201.

[16] T. Abe *et al.* [ISS Detector Working Group], JINST **4** (2009) T05001.

[17] J. S. Berg *et al.* [ISS Accelerator Working Group], JINST **4** (2009) P07001.

[18] See M. Lindroos and M. Mezzetto, "Artificial Neutrino Beams: Beta Beams", Imperial College Press, Aug. 2009, and references therein.

[19] P. Zucchelli, Phys. Lett. B **532** (2002) 166.

[20] R. Battiston, M. Mezzetto, P. Migliozzi and F. Terranova, Riv. Nuovo Cimento, in press; arXiv:0912.3372 [hep-ex].

[21] E. Wildner, "Beta Beam", Talk at the 11th International Workshop on Neutrino Factories, Superbeams and Beta Beams. Information on the EUROν Working package 4: "Beta Beam" are available at `http://www.euronu.org/`.

[22] J. Bernabeu *et al.*, First Yearly Report of the Euroν Working Package 6 (Physics).

[23] J. Bouchez, M. Lindroos and M. Mezzetto, AIP Conf. Proc. **721** (2004) 37; M. Mezzetto, J. Phys. G **29** (2003) 1771; Nucl. Phys. Proc. Suppl. **143** (2005) 309.

[24] A. Donini, E. Fernandez-Martinez, P. Migliozzi, S. Rigolin and L. Scotto Lavina, Nucl. Phys. B **710** (2005) 402.

[25] A. Donini, E. Fernández-Martínez and S. Rigolin, Phys. Lett. B **621** (2005) 276.

[26] J. Burguet-Castell, D. Casper, J. J. Gomez-Cadenas, P. Hernandez and F. Sanchez, Nucl. Phys. B **695** (2004) 217.

[27] J. Burguet-Castell, D. Casper, E. Couce, J. J. Gomez-Cadenas and P. Hernandez, Nucl. Phys. B **725** (2005) 306.

[28] F. Terranova, A. Marotta, P. Migliozzi and M. Spinetti, Eur. Phys. J. C **38** (2004) 69; S. K. Agarwalla, A. Raychaudhuri and A. Samanta, Phys. Lett. B **629** (2005) 33.

[29] P. Huber, M. Lindner, M. Rolinec and W. Winter, Phys. Rev. D **73** (2006) 053002.

[30] A. Donini, E. Fernández-Martínez, P. Migliozzi, S. Rigolin, L. Scotto Lavina, T. Tabarelli de Fatis and F. Terranova, Eur. Phys. J. C **48** (2006) 787.

[31] A. Donini *et al.*, Eur. Phys. J. C **53** (2008) 599.

[32] C. Rubbia, A. Ferrari, Y. Kadi and V. Vlachoudis, Nucl. Instrum. Meth. A **568** (2006) 475.

[33] C. Rubbia, [arXiv:hep-ph/0609235].

[34] A. Donini and E. Fernández-Martínez, Phys. Lett. B **641** (2006) 432.

[35] S. K. Agarwalla, S. Choubey and A. Raychaudhuri, Nucl. Phys. B **771** (2007) 1.

[36] S. K. Agarwalla, S. Choubey and A. Raychaudhuri, Nucl. Phys. B **798** (2008) 124.

[37] P. Coloma, A. Donini, E. Fernandez-Martinez and J. Lopez-Pavon, JHEP **0805** (2008) 050.

[38] A. Jansson, O. Mena, S. J. Parke and N. Saoulidou, Phys. Rev. D **78** (2008) 053002 [arXiv:0711.1075 [hep-ph]].

[39] W. Winter, Phys. Rev. D **78** (2008) 037101.

[40] S. K. Agarwalla, S. Choubey and A. Raychaudhuri, Nucl. Phys. B **805** (2008) 305.

[41] S. K. Agarwalla, S. Choubey, A. Raychaudhuri and W. Winter, JHEP **0806** (2008) 090.

[42] D. Meloni, O. Mena, C. Orme, S. Palomares-Ruiz and S. Pascoli, JHEP **0807** (2008) 115.

[43] S. Choubey, P. Coloma, A. Donini and E. Fernandez-Martinez, JHEP **0912** (2009) 020.

[44] E. Fernandez-Martinez, Nucl. Phys. B **833** (2010) 96.

[45] S. Geer, Phys. Rev. D **57** (1998) 6989 [Erratum-ibid. D **59** (1999) 039903];

[46] The study of this option has been carried out in the framework of the EURISOL Design Study (Task 12: "Beta Beam aspects"). Information are available at `http://beta-beam.web.cern.ch/`.

[47] J. E. Campagne, M. Maltoni, M. Mezzetto and T. Schwetz, JHEP **0704** (2007) 003; M. Marafini, Talk at the 10th Workshop on "Next Generation Nucleon decay and Neutrino Detectors" (NNN09), October 8-10, 2009, Estes Park, Colorado.

[48] "Proton Accelerator for the Future" (PAF) CERN inter-departmental working group webpage, `http://pofpa.web.cern.ch/pofpa/`.

[49] A. Donini and M. Lindroos, *Presented at 10th International Workshop on Neutrino Factories, Superbeams and Betabeams: Nufact08, Valencia, Spain, 30 Jun - 5 Jul 2008*

[50] A. Donini, talk at the CARE04 Workshop, Nov. 2-5, 2004, DESY, Hamburg; http://www-mhf.desy.de/public/care04/2004.11.03 sr2/hampro.pdf

[51] B. Autin *et al.*, J. Phys. G **29** (2003) 1785.

[52] Y. Mori, Nucl. Instrum. Meth. A **562** (2006) 591.

[53] A.N. Skrinsky, V.V. Parkhomchuk, Sov. J. Nucl. Phys. **12** (1981) 3.

[54] O. Tengblad, private communication, http://www.targisol.csic.es/intro database.html

[55] W. T. Winter *et al.*, Phys. Rev. Lett. **91** (2003) 252501.

[56] D. Neuffer *et al.*, Nucl. Instrum. Meth. A **585** (2008) 109.

[57] Information available at `http://paf-ps2.web.cern.ch/paf-ps2/`.

[58] P. Lipari et al., Phys. Rev. Lett. **74** (1995) 4384.

[59] See e.g. S.Y. Lee, "Accelerator Physics", World Scientific, 2004.

[60] M. Mezzetto, Nucl. Phys. Proc. Suppl. **155** (2006) 214 [arXiv:hep-ex/0511005].

[61] M. Benedikt, A. Fabich, S. Hancock and M. Lindroos, Nucl. Phys. Proc. Suppl. **155** (2006) 211. A. Donini, E. Fernández-Martínez, P. Migliozzi, S. Rigolin and L. Scotto Lavina, Nucl. Phys. B **710** (2005) 402.

[62] See `http://beta-beam.web.cern.ch`.

[63] GEANT - Detector Description and Simulation Tool CERN Program Library Long Writeup W5013.

[64] A. Ghezzi, T. Tabarelli de Fatis, G. Tinti and M. Piccolo, "Digital hadron calorimetry with glass RPC active detectors," Contributed to 2005 International Linear Collider Workshop (LCWS 2005), Stanford, California, 18-22 Mar 2005; arXiv:physics/0507021.

[65] M. Ambrosio *et al.*, Nucl. Instrum. Meth. A **456** (2000) 67.

[66] A. Laing and A. Cervera-Villanueva, PoS **NUFACT08** (2008) 042; A. Cervera, F. Dydak and J. Gomez Cadenas, Nucl. Instrum. Meth. A **451** (2000) 123.

[67] J.K. Nelson, "Magnetized iron calorimeters", European Strategy for Future Neutrino Physics Workshop, CERN, Switzerland, 1-3 October 2009.

[68] N. Y. Agafonova et al. [MONOLITH Collaboration], "MONOLITH: A massive magnetized iron detector for neutrino oscillation studies" LNGS-P26-2000, CERN-SPSC-2000-031, CERN-SPSC-M-657.

[69] R. Acquafredda *et al.*, JINST **4** (2009) P04018.

[70] G. Alimonti [Borexino Collaboration] et al., Nucl. Instrum. Meth. A **600** (2009) 568.

[71] P. Huber, M. Lindner and W. Winter, Nucl. Phys. B **645** (2002) 3 [arXiv:hep-ph/0204352].

[72] H. Minakata and H. Nunokawa, JHEP **0110** (2001) 001.

[73] A. Donini, D. Meloni and S. Rigolin, JHEP **0406** (2004) 011.

[74] H. Minakata and S. Uchinami, arXiv:1001.4219 [hep-ph].

[75] T. Tabarelli de Fatis, Eur. Phys. J. C **24** (2002) 43.